

See discussions, stats, and author profiles for this publication at: <https://www.researchgate.net/publication/248841674>

Encapsulated white-light CdSe nanocrystals as nanophosphors for solid-state lighting

ARTICLE *in* JOURNAL OF MATERIALS CHEMISTRY · FEBRUARY 2008

Impact Factor: 7.44 · DOI: 10.1039/b716803a

CITATIONS

59

READS

15

6 AUTHORS, INCLUDING:



[Michael Schreuder](#)

Tetramer Technologies

11 PUBLICATIONS 308 CITATIONS

SEE PROFILE

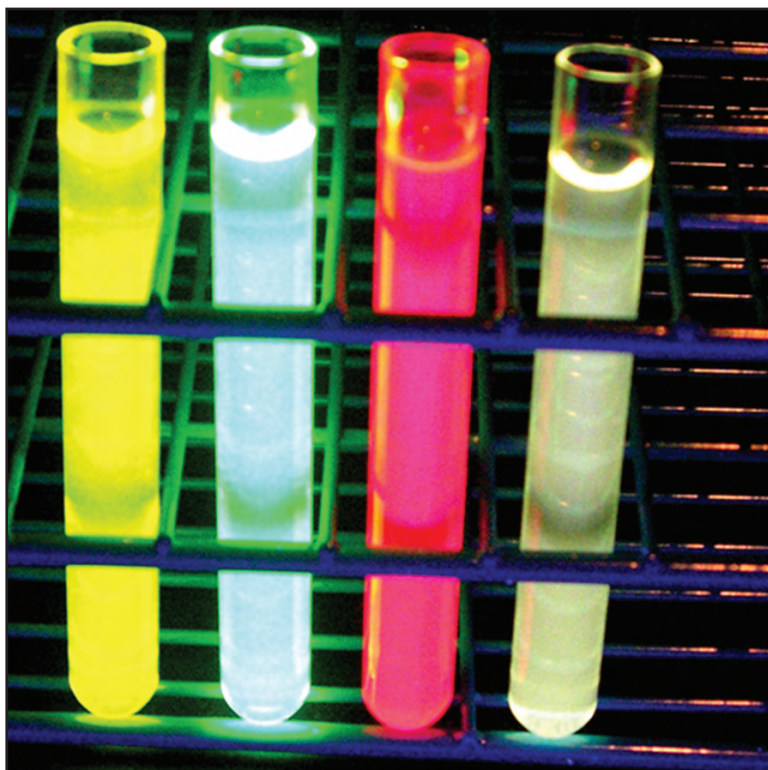


[Jonathan D Gosnell](#)

Vanderbilt University

5 PUBLICATIONS 89 CITATIONS

SEE PROFILE



white-light

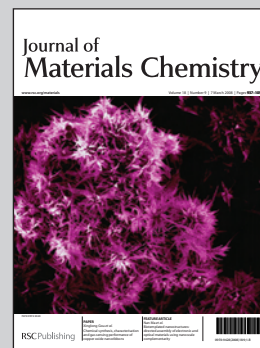
Image reproduced by permission of Sandra Rosenthal

Showcasing research from the Rosenthal and Weiss labs at Vanderbilt University

Title: Encapsulated white-light CdSe nanocrystals as nanophosphors for solid-state lighting

White-light nanocrystals under UV-excitation, in solution (left), encapsulated and coating a flask (right), and spray-painted through a stencil.

As featured in:



See Michael A. Schreuder, Jonathan D. Gosnell, Nathanael J. Smith, Michael R. Warnement, Sharon M. Weiss and Sandra J. Rosenthal, *J. Mater. Chem.*, 2008, **18**, 970

RSC Publishing

www.rsc.org/materials

Registered Charity Number 207890

Encapsulated white-light CdSe nanocrystals as nanophosphors for solid-state lighting

Michael A. Schreuder,^a Jonathan D. Gosnell,^{bc} Nathanael J. Smith,^a Michael R. Warnement,^a Sharon M. Weiss^{bc} and Sandra J. Rosenthal^{*ab}

Received 30th October 2007, Accepted 3rd January 2008

First published as an Advance Article on the web 24th January 2008

DOI: 10.1039/b716803a

White-light emitting ultra-small CdSe nanocrystals present exciting possibilities in the area of solid-state lighting technology. In this work, thirteen dissimilar polymers were examined as potential encapsulants for these single-sized nanocrystals. Films of the encased nanocrystals were characterized in terms of nanocrystal aggregation and changes to the nanocrystals' natural emission. The Hildebrand and Hansen solubility parameters of each encapsulant were found to be correlated to the quality of nanocrystal encapsulation achieved. Encapsulants with cyclosiloxane or bisphenol-A type epoxy structures caused extensive aggregation of the nanocrystals at low loading levels (<0.5% w/w) due to the solubility difference between the polymer structure and the nanocrystals' ligands. Of the encapsulants tested, the most robust, color stable, and homogenous encapsulation was obtained using a biphenylperfluorocyclobutyl polymer. In this polymer, nanocrystal loading levels up to 18% w/w were achieved. White-light emitting CdSe nanocrystals encapsulated in the biphenylperfluorocyclobutyl polymer were coated on various UV-LEDs creating a white light source with chromaticity coordinates of (0.324, 0.322) and a high color-rendering index of 93.

Introduction

Replacing inefficient fluorescent, halogen, and incandescent lighting with solid-state lighting (SSL) could reduce the amount of energy needed for lighting in 2025 by as much as 326 TWH per year (33% of predicted energy needs) and carbon emission by 42 megatons per year in the United States alone.^{1,2} In order to guide this transition from conventional lighting to SSL, the US Department of Energy has proposed the following targets for white SSL for general use: Commission International d'Eclairage (CIE) chromaticity coordinates of pure white light (0.33, 0.33); a high color rendering index (CRI) of >80; and a luminous efficiency (luminous flux output divided by input of electrical power) of 200 lm per watt—although it has been suggested that very high CRI values may limit efficiencies to 145 lm per watt.^{2,3} One proposed SSL solution is the use of semiconductor nanocrystals (NCs) as the emitting layer in either photoluminescent or electroluminescent devices.⁴

In the past, hybrid electroluminescent devices have been fabricated using a single size or multiple sizes of nanocrystals combined with several organic layers to provide either a monochromatic source^{5,6,7} or a solid-state, white-light source.^{8,9} Similarly, most nanocrystal-based photoluminescent devices have used a single-size of nanocrystals combined with a colored LED¹⁰ or a distribution of nanocrystal sizes in a single layer^{11,12} to produce white light. The use of an amber-colored phosphor layer in conjunction with

blue LEDs produces white light that has a halo effect.¹³ In addition, using multiple nanocrystal sizes or phosphor layers to obtain white light leads to complex color mixing. These devices generally suffer from low efficiencies due to self-absorption, scattering, and reflections caused by the various layers.^{11,12} In particular, the use of multiple sizes of nanocrystals (various emission colors¹³) inherently decreases the total emission intensity due to the larger nanocrystals absorbing the emission from the smaller nanocrystals.¹⁴

The use of recently discovered single-size, ultra-small (~1.5 nm diameter) white-light emitting cadmium selenide (CdSe) nanocrystals¹⁵ as a phosphor eliminates the need for multiple phosphor layers, reducing the limitations common in other devices, such as poor efficiencies and low CRI values. These white-light nanocrystals possess a well-balanced broad-spectrum emission that spans the majority of the visible spectrum (Fig. 1, solid red line). Previous work suggesting the use of single-sized broad spectrum cadmium sulfide (CdS) nanocrystals as nanophosphors has been reported;¹⁶ however, neither a CRI, CIE chromaticity coordinates, nor an emission spectrum of the encapsulated nanocrystals were reported.

Encapsulation of white-light emitting CdSe nanocrystals allows for a simple photoluminescent device to be fabricated using a thin layer of encapsulated nanocrystals coated on an ultra-violet (UV) LED (inset, Fig. 1). Encapsulation provides a mechanically stable environment and protection for the nanocrystals against heating and photo-oxidation. Although the temperature on the actual dome of the LED is generally much lower, temperatures inside the junction of UV LEDs have been calculated to reach 140 °C.¹⁷ An optimal encapsulant for the white-light nanocrystals would have no intrinsic emission, prevent nanocrystal aggregation (reducing quenching and scattering), allow ease of application, and provide good adhesion to UV LED surfaces.^{18,19}

^aDepartment of Chemistry, Vanderbilt University, Station B 351824, Nashville, TN, 37235, USA. E-mail: sandra.j.rosenthal@vanderbilt.edu; Fax: +1 615-343-1234; Tel: +1 615-322-2633

^bInterdisciplinary Graduate Program in Materials Science, Vanderbilt University, Station B 351824, Nashville, TN, 37235, USA

^cDepartment of Electrical Engineering and Computer Science, Vanderbilt University, Station B 351824, Nashville, TN, 37235, USA

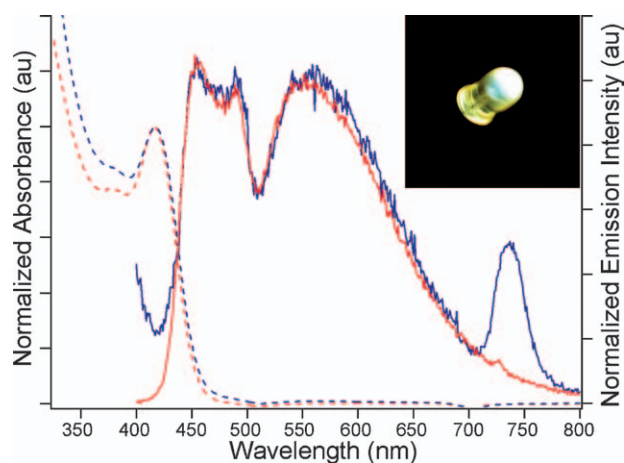


Fig. 1 Absorbance and emission of CdSe white-light nanocrystals. The dashed lines are absorbance spectra, while the continuous lines show the emission of the nanocrystals. The red spectra are nanocrystals solvated in toluene; the blue spectra are 12% w/w nanocrystals in biphenylperfluorocyclobutyl polymer (BP-PFCB). The feature at 400 nm (blue solid line) is an artifact due to the tail of the excitation source's emission, and the emission feature at 730 nm is a 2nd order diffraction peak introduced by the detection setup. The inset is a true color photograph of a 365 nm LED coated with encapsulated nanocrystals.

Table 1 The thirteen encapsulants examined, along with the type of encapsulant and supplier of each. The type of encapsulant is defined by the structures (Fig. 2).

Corporation or supplier	Trade name	Type of encapsulant
Environment. Tech. Inc.	Easy Cast	Epoxy
Environment. Tech. Inc.	Castin' Craft	Polyester
Epoxy Technologies	EpoTek 301-2	Epoxy
Insulcast	510 PTA-B	Silicone
Insulcast	RTVS61	Silicone
Aptek Labs	6100-1AB	Epoxy
Resinlab/Ellsworth Adh.	EP965LVLX clear	Epoxy
Resinlab/Ellsworth Adh.	EP961 clear	Epoxy
Halocarbon Prod. Corp.	Series 40	Halowax
Halocarbon Prod. Corp.	Series 2300	Halowax
Artmolds	Aqua Clear	Epoxy
GE Silicones	TSE3033	Silicone
Tetramer Technologies, L.L.C	Biphenyl-PFCB	Thermoplastic fluoro-carbon chain polymer

Thirteen different encapsulants (Table 1), all optically clear and having dissimilar chemical composition, were examined to determine which would best meet the criteria necessary for a nanocrystal encapsulant. The generalized structures of the various types of encapsulants can be seen in Fig. 2. These contrasting structures proved to have a significant impact on the quality of the nanocrystal encapsulation for each polymer.

Experimental

Nanocrystal synthesis and encapsulation

Single-sized, white-light CdSe nanocrystals were synthesized as previously reported¹⁸ and solvated in toluene. Generally the nanocrystal concentration was around 2% w/w, to avoid aggregation prior to encapsulation. This synthesis yields nanocrystals

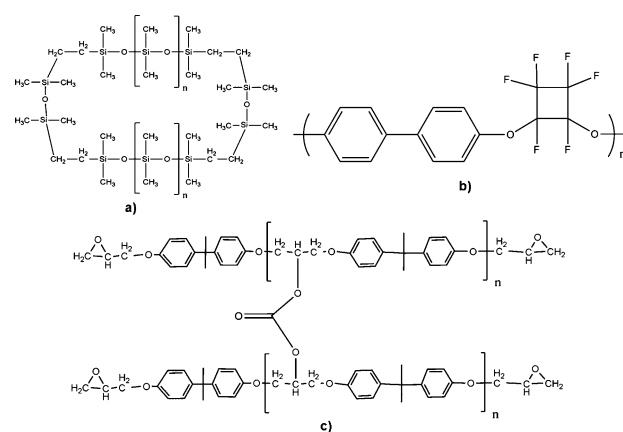


Fig. 2 a) Structure of siloxane polymers. b) Biphenylperfluorocyclobutyl polymer repeat unit (BP-PFCB) c) Structure of epoxy polymers, also known as diglycidyl ether of bisphenol A polymers.

coated with dodecylphosphonic acid (DDPA) and tri-*n*-octylphosphine oxide (TOPO) with quantum yields from 6 to 10%.

Each encapsulant was prepared according to the instructions provided by the manufacturer. For the siloxanes, epoxies, and the polyester polymer, this involved mixing specific volumes or weights of two components; the halowaxes were melted; and the biphenylperfluorocyclobutyl polymer (BP-PFCB) was suspended in mesitylene at 20% w/w.

The solvated nanocrystals were mixed with each encapsulant, and thin films (10 to 50 μ m) of the encapsulated nanocrystals were deposited on glass slides or in molds, and cured according to the specific guidelines of each encapsulant.

Characterization

Absorption and photoluminescence measurements were performed for the various encapsulants with and without nanocrystals. Film thicknesses were determined using an Aerospace IP54 electronic micrometer and a Veeco DekTak 150 profilometer. Absorption measurements were conducted on a Varian-Cary 50 Bio UV-visible spectrophotometer. Fluorescence microscopy, used to monitor aggregation, was conducted on a Zeiss Axiovert 200 M inverted fluorescence microscope equipped with a Photometrics Coolsnap HQ2 CCD camera and Metamorph image acquisition software. The photoluminescence measurements were made using a 365 nm LED as an excitation source (chosen to discriminate the excitation LED light from the nanocrystal emission) and an ISS PC1 photon-counting spectrometer (Fig. 3). This setup was used specifically for detection of emission intensities and emission spectral characteristics. A Labsphere SLMS-LED-1050 integrating sphere system, fiber coupled to a CDS 500 CCD-based spectrometer with accompanying software was used to determine the luminous efficiency, CIE chromaticity coordinates, and the CRI of each 365 nm LED coated with encapsulated white-light nanocrystals.

Results and discussion

Encapsulation differences

As seen in Fig. 4, only BP-PFCB and TSE 3033 did not significantly quench the emission from the white-light nanocrystals.

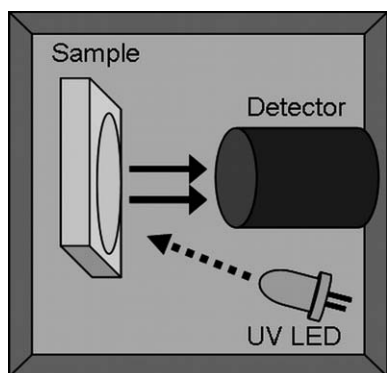


Fig. 3 Configuration for photoluminescence of encapsulated nanocrystal films. The emission from a 365 nm LED (dotted arrow) was used to excite encapsulated CdSe nanocrystals, which emit white light (solid arrows) back to the detector, a photon-counting spectrometer. This setup was chosen to spectrally and spatially differentiate the excitation light from the nanocrystals' emission.

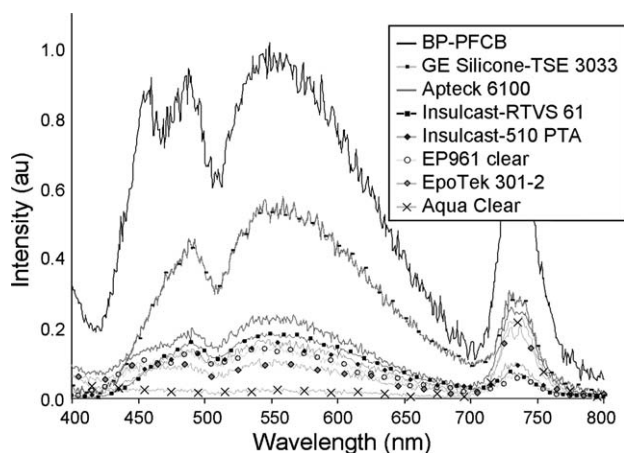


Fig. 4 The emission from ultra-small single-sized nanocrystals in various encapsulants. The samples were all $50 \pm 3 \mu\text{m}$ thick films and at 9% w/w nanocrystal to polymer loading.

Of these two encapsulants, only BP-PFCB maintained the unique absorption and emission spectra of these broad spectrum nanocrystals (Fig. 1). The main alternative to BP-PFCB, TSE 3033, provided less than half the overall emission intensity as a BP-PFCB film with the same nanocrystal w/w percent loading and thickness. The remaining encapsulants shown in Fig. 4 not only emitted at less than 25% of the intensity achieved with BP-PFCB, but also altered the emission spectrum of the nanocrystals. The spectral modifications can be noted most easily through the absence or decreased intensity of the emission peak at 455 nm. It can be seen in Fig. 4, that in general the epoxies quenched the nanocrystal emission more than siloxanes, and both the epoxies and siloxanes quenched the emission intensity a great deal more than BP-PFCB. In addition, many of the other encapsulant films were not as robust as the BP-PFCB films. When the encapsulated nanocrystal films were annealed at 190°C for 48 hours, most became extremely discolored and the emission of the nanocrystals decreased to an almost unobservable level in all but the BP-PFCB, TSE 3033, and RTVS61.

The disparity in emission intensity seen in the diverse encapsulants is due to the nanocrystals aggregating to varying degrees in each polymer. White-light fluorescence images (Fig. 5) clearly show this aggregation. Siloxane encapsulants caused the largest nanocrystal aggregates ($\sim 10 \mu\text{m}$ in diameter, Fig. 5a), with a micelle-like structure. These large aggregates appeared to quench the nanocrystals less than the epoxy polymers. The epoxy encapsulants caused much smaller aggregates to form ($\sim 1 \mu\text{m}$ in diameter, Fig. 5b), quenching a large part of the emission intensity. Monodisperse nanocrystal encapsulation was only achieved in BP-PFCB (Fig. 5c). The fluorescence from these encapsulated nanocrystals was not only much more intense than in the other encapsulants, but also maintained its spectral purity (Fig. 1 and Fig. 4).

The aggregation differences in each of the encapsulants can be traced back to the structure. The assorted structures provide a unique Hildebrand solubility parameter (δ). This Hildebrand solubility parameter can be separated into Hansen's solubility parameters (HSPs), as seen by eqn 1. These three parameters relate the atomic/dispersive interactions (δ_D), dipole-dipole interactions (δ_P), and hydrogen bonding interactions (δ_H).²⁰ These parameters are commonly used to determine the interactions between solutes and solvent systems.²⁰ The more similar the Hansen solubility parameters between the solute and solvent, the more likely the two are to combine. This holds true for polymer-liquid and solute-polymer interactions as well. Table 2 shows the solubility parameters for some common solvents and representative encapsulants examined. Toluene is used to provide representative values for the nanocrystals and mesitylene is considered representative for BP-PFCB, although more work is required to fully confirm these values.

$$\delta^2 = (\delta_D)^2 + (\delta_P)^2 + (\delta_H)^2 \quad (1)$$

Three of the encapsulants tested were siloxane polymers: TSE3033, RTVS61, and 510 PTA-B. The backbones of the siloxane polymers are more polar than toluene (a good solvent for the nanocrystals), however the methyl side-chains on the repeat unit (Fig. 2a) give these siloxane polymers an overall Hildebrand solubility parameter of $14.9\text{--}17.5 \delta(\text{SI})$,²⁰ similar to toluene's Hildebrand value of $18.2 \delta(\text{SI})$.²⁰ However, the differences between the HSPs for toluene and for the siloxanes indicate that these polymers are inappropriate for use with the nanocrystals, due to the extremely polar silicon-oxygen bonds.²¹

Six of the encapsulants typify bisphenol-A epoxies (EasyCast, EpoTek 301-2, 6100-1AB, EP965LVLX, EP961, and Aqua-Clear). These polymer backbones are relatively less polar than siloxanes and should mix well with the nanocrystals in toluene. However, as can be seen in Fig. 2c the end-group on the polymer is an epoxide and the cross-linking group is an acrylate. This combination of polar and non-polar functional groups gives epoxies Hildebrand solubility parameters of $18\text{--}26 \delta(\text{SI})$.²⁰ Additionally, the δ_P and δ_H for epoxies are significantly higher than the solvents generally used with these nanocrystals (Table 2).²² Therefore, the epoxies are not an appropriate choice of encapsulant for the nanocrystals.

The biphenylperfluorocyclobutyl polymer (BP-PFCB), commercially available from Tetramer Technologies, L.L.C., was the most effective encapsulant found due to its unique structure

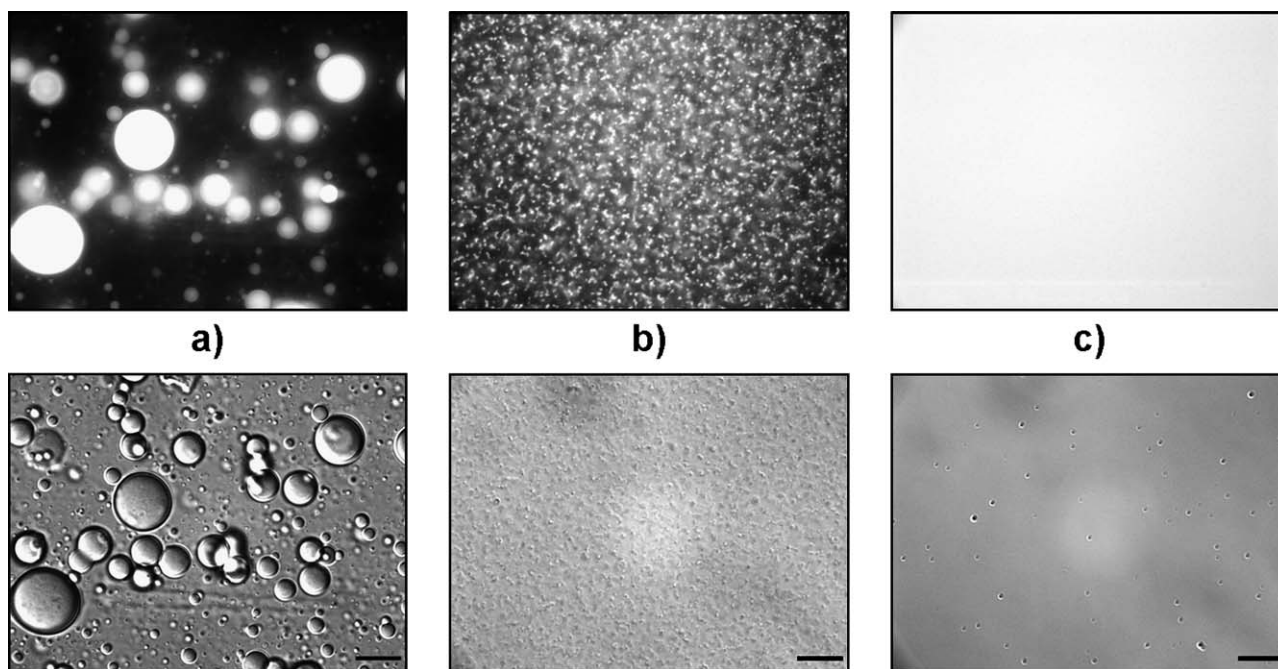


Fig. 5 Representative white-light fluorescence (top) and bright field differential interference contrast (bottom) micrographs of encapsulated nanocrystals at 5% w/w loading in: a) siloxane b) epoxy c) BP-PFCB. All images were acquired with an exposure time of 5 ms, displayed with equivalent thresholds, and at the same thickness ($\sim 2 \mu\text{m}$). The scale bars represent $10 \mu\text{m}$ on all the images. The uniform fluorescence illustrated in c) is representative of disperse nanocrystal fluorescence in BP-PFCB and is not an artifact due to overexposure of the image.

Table 2 Hildebrand solubility parameter for various polymers and solvents of interest are shown. Representative Hansen values are shown for the various types of polymers and solvents. Methanol is included to provide contrasting values, as the nanocrystals are insoluble in it. All the parameters should be taken into consideration when assessing possible encapsulants.^a

Encapsulant or solvent	$\delta(\text{SI})$	$\delta_{\text{D}}(\text{SI})$	$\delta_{\text{P}}(\text{SI})$	$\delta_{\text{H}}/\text{SI}$
Methanol	29.6	15.1	12.3	22.3
Toluene ^b	18.2	18.0	1.4	2.0
Mesitylene ^c	18.0	18.0	0.0	0.6
Epoxies	18–26	18.3	12.3	9.7
Siloxanes	14.9–17.5	16.4	1.6	7.8

^a All values were taken from ref. 20–22. ^b The values for toluene are good representatives for the solubility values for the nanocrystals. ^c Mesitylene provides a good approximation for the BP-PFCB values.

(Fig. 2b). The Hildebrand value of BP-PFCB, estimated to be similar to that of mesitylene (18.0), is very similar to that of toluene. Additionally, the HSPs for mesitylene are notably more similar to those of toluene than those for siloxanes and epoxies (Table 2). This combination of solubility parameters explains why BP-PFCB causes less aggregation than the other polymers tested.

Characteristics of nanocrystals in BP-PFCB

As seen in Fig. 1, the nanocrystals encapsulated in BP-PFCB have almost identical absorption and emission spectra as prior to encapsulation. This suggests that the size distribution of the nanocrystals is not changed and very little nanocrystal aggregation is occurring during the encapsulation process. CIE chromaticity coordinates for the sample shown in Fig. 1 in solution

(0.326, 0.342) were only slightly changed when encapsulated in BP-PFCB (0.328, 0.349), both falling well within the limits of white light as defined by the CIE.²³ The nanocrystals' quantum yield (6% to 10%) was not affected by the encapsulation. The quantum yields of the films were determined in a manner similar to Greenham *et al.*²⁴ Moreover, BP-PFCB encapsulated nanocrystals maintained at 190°C for 48 hours showed very little change in spectral characteristics, indicating that BP-PFCB allows the nanocrystals to withstand temperatures nearly double the standard operating temperature normally attained by LEDs. The retention of spectral features, a priority for making devices, shows the protection afforded by BP-PFCB against heating, as nanocrystals in solution would aggregate and sinter at these temperatures.

Structural impacts on other encapsulants

Encapsulants not shown in Fig. 4 did not appropriately mix with the nanocrystals. This was seen in three ways: improper curing of the encapsulant, non-uniform nanocrystal dispersion in the films, or visible modification of the nanocrystals. These problems could all be traced back to structural differences in the polymers or the components used to cure them. The Castin' Craft polyester encapsulant contained a peroxide hardener which quickly oxidized the nanocrystals, eliminating any absorbance or fluorescence. The Series 40 and 2300 Halowaxes had melting points that prohibited nanocrystal encapsulation. The Series 40 wax is a liquid at room temperature, while the melting point of the Series 2300 ($>132^\circ\text{C}$) is greater than the boiling point of toluene. The remaining encapsulants, EP965LVLX and EasyCast did not cure according to schedule, due to the acrylate hardener and excess DDPA, from the nanocrystal synthesis participating in

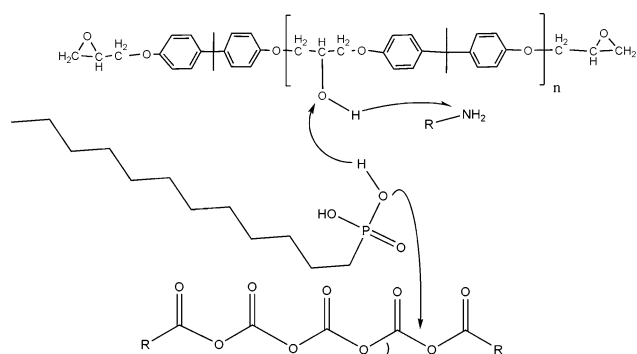


Fig. 6 Nucleophilic substitution of DDPA onto an epoxy's acrylate hardener. Note that although this is shown as a concerted reaction, this occurs in a number of steps.

a nucleophilic substitution (Fig. 6). It is likely that these two epoxy encapsulants, if cured properly, would have exhibited similar nanocrystal aggregation as the other epoxy polymers.

Nanocrystal loading and sample thickness

BP-PFCB, clearly the best encapsulant, was used to study the effect of nanocrystal loading and sample thickness. Over the thickness range considered (10 to 50 μm), no change in spectral shape was detected, while the emission intensity was linearly proportional to the thickness. Changes to the nanocrystal loading also did not modify the spectrum of emitted light; however, the emission intensity increases sharply as the nanocrystal loading increases from 5 to 9% w/w (Fig. 7). Below 5% w/w loading, the emission intensity appears to be linear; however, this could be due to the detection limits of our measurement system. Increased nanocrystal loading above 9% w/w does not have as significant an effect on the emission intensity and almost fully plateaued around 18% w/w. Chosen as representative siloxane and epoxy encapsulants, Insulcast-RTVS61 and EpoTek 301-2 exhibited a similar trend in changes to the emission intensity. However, their emission intensity plateaued at much lower nanocrystal concentrations (0.36 and 0.25%, respectively). This

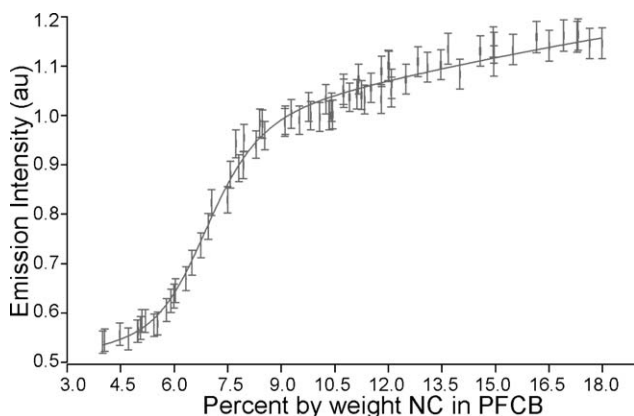


Fig. 7 Emission intensity of CdSe white-light nanocrystals in BP-PFCB vs. percent by weight loading. The data shown in this graph is from thin films studied using the setup in Fig. 2. The line drawn is meant only as a guide for the eye.

plateauing is due to the nanocrystals aggregating past a certain loading.

Nanophosphor devices built using BP-PFCB

Devices fabricated using BP-PFCB encapsulated nanocrystals presented some impressive results. The CIE chromaticity coordinates for a 365 nm emitting LED coated with a nanophosphor layer were (0.324, 0.322), with a measured CRI of 93. These values are superior to several commercially available LEDs.²⁵

Preliminary luminous efficiency results obtained for various coated LEDs range from 0.19 lm per watt to just below 1 lm per watt. This is below the projected goal of the DOE for SSL; however, significant improvements can be attained with further optimization of these prototype devices. This progress can be realized in various ways: increasing the nanocrystals' quantum yield (currently 6 to 10%), increasing the low UV LED efficiency (currently ~5 to 10%), using higher wavelength LEDs to reduce the Stokes loss, and increasing the light-extraction efficiency through improved device geometry.

Conclusions

In this work, ultra-small white-light CdSe nanocrystals were encapsulated in various polymers. A correlation between the Hildebrand parameter and the HSPs of the various encapsulants and their effectiveness at encapsulating these nanocrystals was found. This correlation is for nanocrystals with these particular ligands; nanocrystals with different ligands may show a preference to other polymers. Experimentally, of the thirteen encapsulants studied only BP-PFCB represents a practical option for encapsulation, creating a rugged, color-stable environment for the white-light nanocrystals. This encapsulation in BP-PFCB allowed the nanocrystals to be combined with UV LEDs to create a potentially viable, solid-state white-light source. Initial attempts at coating UV LEDs were successful in meeting two out of three DOE goals for general illumination by exhibiting CIE chromaticity coordinates (0.324, 0.322) and a CRI of 93. Having already surpassed several commercial devices in color quality, future developments will be aimed at improving the luminous efficiency of our white-light CdSe nanophosphor devices to a commercially realistic number.

Acknowledgements

This work was supported by a Vanderbilt University Discovery Grant and the US Department of Energy. JDG was supported by a NSF Integrated Graduate Education and Research Training program. Advice and BP-PFCB samples from Dr Jianyong "Jack" Jinn and Dr Earl Wagner at Tetramer Technologies, L.L.C. are gratefully acknowledged.

References

- 1 J. R. Brodrick, *Energy Savings Potential of SSL in General Illumination Applications*, Report for US Department of Energy, Navigant Consulting Inc., Washington DC, 2003.
- 2 *Building Energy Data Book 2006*. US Department of Energy. Silver Spring, MD, USA, November 21, 2006, <http://buildingsdatabook.eren.doe.gov>.

- 3 J. Y. Tsao, *Light Emitting Diodes (LEDs) for General Illumination*, Optoelectronics Industry Development Association, Washington DC, 2002.
- 4 A. D. Yoffe, *Adv. Phys.*, 2001, **50**, 1.
- 5 V. L. Colvin, M. C. Schlamp and A. P. Alivisatos, *Nature*, 1994, **370**, 354.
- 6 S. Coe-Sullivan, W.-K. Woo, J. S. Steckel, M. Bawendi and V. Bulovic, *Org. Electron.*, 2003, **4**, 123.
- 7 M. Achermann, M. A. Petruska, S. Kos, D. L. Smith, D. D. Koleske and V. I. Klimov, *Nature*, 2004, **429**, 642.
- 8 Y. Li, A. Rizzo, M. Mazzeo, L. Carbone, L. Manna, R. Cingolani and G. Gigli, *J. Appl. Phys.*, 2005, **97**, 113501.
- 9 Y. Li, R. Cingolani and G. Gigli, *Adv. Mater.*, 2006, **18**, 2545.
- 10 A. V. Firth, D. J. Cole-Hamilton and J. W. Allen, *Appl. Phys. Lett.*, 1999, **75**, 3120.
- 11 J. Lee, V. C. Sundar, J. R. Heine, M. G. Bawendi and K. F. Jensen, *Adv. Mater.*, 2000, **12**, 1102.
- 12 H. S. Chen, S. J. J. Wang, C. J. Lo and J. Y. Chi, *Appl. Phys. Lett.*, 2005, **86**, 131905.
- 13 L. Brus, *J. Chem. Phys.*, 1983, **79**, 5566; L. Brus, *J. Chem. Phys.*, 1984, **80**, 4403; T. Kippeny, L. A. Swafford and S. J. Rosenthal, *J. Chem. Educ.*, 2002, **79**, 1094.
- 14 F. K. Yam and Z. Hassan, *Microelectron. J.*, 2005, **36**, 129.
- 15 M. J. Bowers II, J. R. McBride and S. J. Rosenthal, *J. Am. Chem. Soc.*, 2005, **127**, 15378.
- 16 L. E. Shea-Rowher, B. L. Abroms, J. P. Wilcox and S. G. Thomas, *Proc. SPIE-Int. Soc. Opt. Eng.*, 2004, **66**, 5366.
- 17 Y. Xi, T. Gessmann, J. Xi, J. K. Kim, J. M. Shah, E. F. Shubert, A. J. Fisher, M. H. Crawford, K. H. A. Bogart and A. A. Allerman, *Jpn. J. Appl. Phys.*, 2005, **44**, 7260.
- 18 J. D. Gosnell, M. A. Schreuder, M. J. Bowers II, S. J. Rosenthal and S. M. Weiss, *Proc. SPIE-Int. Soc. Opt. Eng.*, 2006, **6337**, 63370A.
- 19 G. Chen, R. Rapaport, J. Jin, T. Floyd and E. Wagener, *Polym. Prepr.*, 2006, **47**(2), 1012.
- 20 A. F. M. Barton, *CRC Handbook of Polymer-Liquid Interaction Parameters and Solubility Parameters*, ed. A. F. M. Barton, CRC Press, Boca Raton, 2000; C. M. Hansen, in *Hansen Solubility Parameters (A User's Handbook)*, ed. C. M. Hansen, CRC Press, Boca Raton, 2000.
- 21 A. F. M. Barton, in *CRC Handbook of Solubility Parameters and Other Cohesion Parameters*, ed. A. F. M. Barton, CRC Press, Boca Raton, 1991, ch. 14; R. H. Baney, C. E. Voigt and J. W. Mentele, in *Structure-Solubility Relationship in Polymers*, ed. F. W. Harris and R. B. Seymour, Academic Press, New York, 1977, pp. 228–231; L. N. Lewis, in *Silicones and Silicone-Modified Materials*, ed. S. J. Clarson, J. J. Fitzgerald, M. J. Owen and S. D. Smith, Oxford University Press, Oxford, 2000, ch. 2, pp. 11–19.
- 22 S. H. Goodman, in *Handbook of Thermoset Plastics*, ed. S. H. Goodman, Noyes Publication, Park Ridge, 1986, ch. 6; R. H. Baney, C. E. Voigt and J. W. Mentele, in *Structure-Solubility Relationship in Polymers*, ed. by F. W. Harris and R. B. Seymour, Academic Press, New York, 1977, pp. 228–231.
- 23 CIE, *Commission Internationale de l'Eclairage Proceedings*, 1931, Cambridge University Press, Cambridge.
- 24 N. C. Greenham, I. D. W. Samuel, G. R. Hayes, R. T. Phillips, Y. A. R. R. Kessener, S. C. Moratti, A. B. Holmes and R. H. Friend, *Chem. Phys. Lett.*, 1995, **24**, 89.
- 25 Values for three commercially available “white” LEDs (CoolerGuys: 3 mm, 5 mm, 5 mm ultra-bright): CIE chromaticity coordinates = (0.256, 0.251), (0.243, 0.234), and (0.298, 0.321); CRI = 80.2, 75.7, and 73.0.